

Temperature-dependent Raman spectroscopy in BaRuO_3 system s

Y .S .Lee

Center for Strongly Correlated Materials Research,
Seoul National University, Seoul 151-747, Korea

T .W .Noh

School of Physics and Research Center for Oxide Electronics,
Seoul National University, Seoul 151-747, Korea

J .H .Park and K .B .Lee

Department of Physics, Pohang University of Science and Technology, Pohang,
KoreaG .Cao^z and J .E .CrowNational High Magnetic Field Laboratory, Florida State University,
Tallahassee, Florida 32306

M .K .Lee and C .B .Eom

Department of Material Science and Engineering, University of
Wisconsin-Madison, Madison, Wisconsin 53706E .J .Oh and In-Sang Yang^yDepartment of Physics, Ewha Womans University, Seoul 120-750, Korea
(January 1, 2022)

We investigated the temperature-dependence of the Raman spectra of a nine-layer BaRuO_3 single crystal and a four-layer BaRuO_3 epitaxial film, which show pseudogap formations in their metallic states. From the polarized and depolarized spectra, the observed phonon modes are assigned properly according to the predictions of group theory analysis. In both compounds, with decreasing temperature, while A_{1g} modes show a strong hardening, E_g (or E_{2g}) modes experience a softening or no significant shift. Their different temperature-dependent behaviors could be related to a direct Ru metal bonding through the face-sharing of RuO_6 . It is also observed that another E_{2g} mode of the oxygen participating in the face-sharing becomes split at low temperatures in the four layer BaRuO_3 . And, the temperature-dependence of the Raman continua between $250 - 600 \text{ cm}^{-1}$ is strongly correlated to the square of the plasma frequency. Our observations imply that there should be a structural instability in the face-shared structure, which could be closely related to the pseudogap formation of BaRuO_3 systems.

PACS number : 78.30.-j, 63.20.-e, 71.45.Lr

I. INTRODUCTION

Recently, it was reported that a pseudogap formation can occur in 4d transition metal oxides, BaRuO_3 compounds.^{1,2} Optical conductivity spectra $\sigma_1(\omega)$ of both four-layer hexagonal (4H) BaRuO_3 and nine-layer rhombohedral (9R) compounds show clear electrodynamic response changes resulting from the pseudogap formation. In their metallic states, concurrent developments of a gap-like feature and a coherent mode below a gap-like feature are observed due to the partial-gap opening in the Fermi surface.

The pseudogap formations in the ruthenates could be closely related to their structures characterized by hexagonal close-packing. As shown in Fig. 1, their layered structures include the face-sharing structure of RuO_6 octahedra along the c-axis. In 4H and 9R struc-

tures, two and three adjacent RuO_6 octahedra participate in face-sharing, respectively. A direct Ru-Ru metal bonding formed through such face-sharing distinguishes their physical properties from those of the perovskite ruthenates only with the Ru-O-Ru interaction through corner-sharing.³ Actually, the metal bonding has been seen to be closely related to interesting physical properties, such as a metal-insulator transition in Ti_2O_3 ⁴ and non-Fermi liquid behavior in $\text{La}_4\text{Ru}_9\text{O}_{16}$.⁵ In the case of BaRuO_3 systems, the quasi-one-dimensional (1D) Ru metal bonding along the c-axis might induce a charge density wave (CDW) instability. It was reported that a 5d transition metal oxide 9R BaIrO_3 , which is expected to have stronger metal bonding character than 9R BaRuO_3 due to a more extended 5d-orbital character, shows a static CDW instability.⁶ For BaMO_3 ($M = \text{Ru}, \text{Ir}$) with 9R or 4H structure, it was observed that the

strength of the metalbonding through the face-sharing should be a parameter in determining their physical properties.² These strongly indicate that a CDW instability could be related to the pseudogap formation in the BaRuO₃ systems.

In usual 1D density wave systems, a static CDW ordering state accompanies a structural distortion with a metal-insulator transition. When Peierls-type lattice distortion occurs, in general, new phonon modes in infrared (IR) and Raman spectra can be observed due to structural symmetry breaking. This could also result in a superlattice or an additional peak in x-ray diffraction (XRD) patterns or neutron scattering experiments. In the case of BaRuO₃ systems, although a 1D-like CDW instability is strongly suggested, there has been no structural report about structural distortions.⁷ These might be related to a fluctuation-type instability without any static CDW ordering.

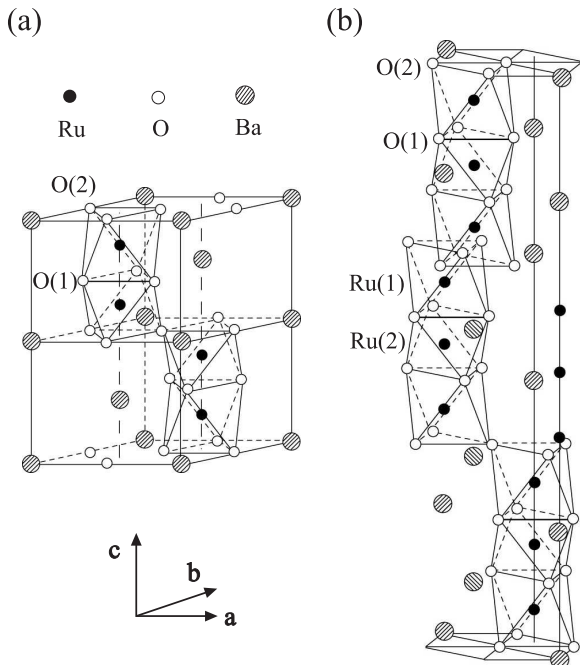


FIG. 1. Schematic diagrams of the two crystallographic forms of BaRuO₃; (a) 4H phase, (b) 9R phase. The arrows represent the crystallographic axes. The details are described in the text.

When the time scale of CDW fluctuations is long enough to induce a pseudogap formation in $\gamma_1(!)$, a phonon anomaly, such as the creation or splitting of a phonon, can be observed.^{8,11} In the metallic state of BaRuO₃ compounds, the screening of free carriers makes the detailed analysis of IR-active phonons difficult. On the other hand, Raman spectroscopy is known to be less affected by free-carrier responses than IR spectroscopy. So, Raman spectroscopy could be a useful tool to address the origin of pseudogap formation of BaRuO₃ compounds in view of their structural properties.

In this paper, we report the Raman spectra of 4H and 9R BaRuO₃ compounds. According to group theory analysis, the observed phonon modes are properly assigned. From the temperature (T)-dependent experiments, it is observed that the T-dependent behavior of phonons strongly depends on the vibrational directions, which could be related to the structural characteristics with the face-sharing of RuO₆ octahedra. Interestingly, the E_{2g} mode of the face-shared oxygen in 4H BaRuO₃ becomes split with decreasing T. These observations indicate that there should be a structural instability due to the metalbonding through the face-sharing of RuO₆ octahedra, which could be closely related to the pseudogap formation in these ruthenates.

II. EXPERIMENTALS

4H BaRuO₃ epitaxial film on (111) SrTiO₃ substrate was fabricated by a 90° ϕ -axis sputtering technique.¹² Its thickness is about 3200 Å. XRD and transmission electron microscopy reveal that the film is composed of a high quality single domain with a c-axis structure. 9R BaRuO₃ single crystal was prepared by a flux-melting method.¹³ The size of the sample is 0.5 × 0.5 × 0.2 mm³. XRD measurements showed that the c-axis was pointing along the short dimension. Due to the size limitation, most Raman spectra were obtained in the ab-plane.

Raman scattering measurements were performed in the backscattering geometry using a triple Raman spectrometer (Jobin Yvon T64000). The incident laser beam was the 514.5 nm line of an Ar-ion laser and the laser power was about 3.6 mW on the sample surface. Raman spectra were measured at various T between 5 K and 650 K. Below 300 K, a continuous flow type of cryostat was used. Above 300 K, a home-made sample heating system was used. Due to the heating effect of the focused laser, the assigned temperatures in this paper could be slightly different from the actual ones on the measured sample surface. At all T, polarized and depolarized spectra were obtained and corrected by a Bose-Einstein factor. The details are described elsewhere.¹⁴

III. RESULTS AND DISCUSSIONS

A. Group theory analysis and phonon assignment

The 4H structure has D_{6h} symmetry,^{15,16} and four molecular units in the primitive cell with eight Raman-active modes (2A_{1g} + 2E_{1g} + 4E_{2g}), twelve IR-active modes (5A_{2u} + 7E_{1u}) and eighteen silent optic modes (A_{2g} + A_{1u} + 3B_{1g} + 2B_{1u} + 5B_{2u} + 6E_{2g}). The Raman-active modes are composed of E_{2g} of Ba, A_{1g}, E_{1g}, and E_{2g} of Ru, and A_{1g}, E_{1g}, and 2E_{2g} of O. The point group for the 9R structure is D_{3d},^{15,16} with three

molecular units in the primitive cell. A factor group analysis predicts nine Raman-active modes ($4A_{1g} + 5E_g$), sixteen IR-active modes ($7A_{2u} + 9E_u$), and three silent optic modes ($2A_{1u} + A_{2g}$). The Raman-active modes are composed of A_{1g} and E_g of Ba, A_{1g} and E_g of Ru, and $2A_{1g}$ and $3E_g$ of O.

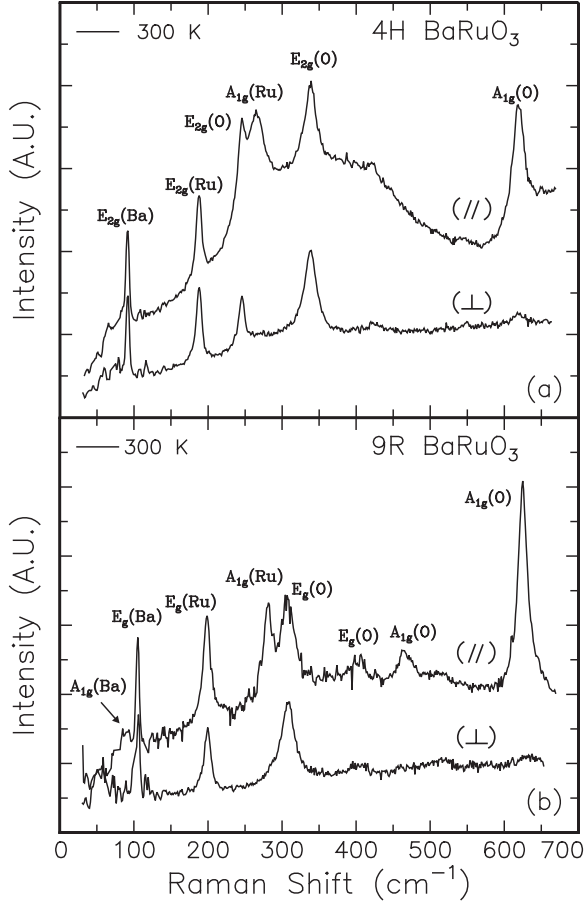


FIG. 2. Polarized (//) and depolarized (⊥) Raman spectra of (a) 4H and (b) 9R BaRuO₃ in the ab-plane at 300 K.

It is noted that only the O ions participating in the face-sharing and only the Ru ions in RuO₆ octahedra participating in the corner-sharing have Raman-active phonon modes. O ions in both ruthenates are positioned at two irreducible sites, i.e. a face-shared plane and an edge in RuO₆ blocks, represented by O (1) and O (2) respectively, in Fig. 1. From the group analysis, O (2) should have only the IR-active phonon modes ($A_{2u} + 2E_{1u}$ for 4H BaRuO₃ and $2A_{2u} + 3E_u$ for 9R BaRuO₃), while O (1) should have both IR- and Raman-active modes. Unlike 4H BaRuO₃, 9R BaRuO₃ has two irreducible Ru-ion sites, i.e. a side and a center position in the RuO₆ blocks, represented by Ru (1) and Ru (2) in Fig 1 (b). Similarly to the case of O ions, Ru (2) should have the IR-active phonon modes ($A_{2u} + E_u$) only. So, it is expected that 4H and 9R BaRuO₃ show similar Raman-active phonon spectra in spite of the different layered structures. For

convenience, we will abbreviate O (1) and Ru (1) to O and Ru, respectively.

Figure 2 (a) shows the polarized and depolarized spectra of 4H BaRuO₃. Six phonon peaks are observed in the polarized spectra. In the depolarized spectra, four peaks are observed at the same frequency positions with the corresponding phonons in the polarized spectra. Note that both the A_{1g} and the E_{2g} modes in the D_{6h} symmetry contribute to the polarized signal, but only the E_{2g} modes are present in the depolarized spectra, which is an indicator for assigning the observed phonon modes.¹⁷ So, four modes observed in depolarized spectra can be assigned as E_{2g} modes. Generally, the phonon frequencies related to the vibration of heavier ions are lower than those of lighter ions. Thus, the four modes in ascending order of their frequency are assigned as one E_{2g} (Ba), one E_{2g} (Ru) and two E_{2g} (O). The rest of the modes in the polarized spectra are assigned as A_{1g} (Ru) and A_{1g} (O) from the lowest frequency. Note that according to the predictions of group theory, two E_{1g} modes of Ru and O cannot be observed in Raman spectra from the ab-plane of the thin film sample.

The observed phonons in 9R BaRuO₃ are assigned in a similar way. As shown in Fig. 2 (b), eight phonons are observed in the polarized spectra. And, three clear modes, which are assigned as E_g (Ba), E_g (Ru) and E_g (O), are observed in the depolarized spectra. Though the mode near 403 cm⁻¹ in the polarized spectra is not clearly observed in the depolarized spectra at 300 K, a distinguishable feature of this mode is detected in the depolarized spectra at low T. So, the mode is assigned as another E_g (O) mode. The rest of the modes in ascending order of their frequency in the polarized spectra are assigned as A_{1g} (Ba) near 85 cm⁻¹, A_{1g} (Ru) near 280 cm⁻¹, and two A_{1g} (O) near 463 cm⁻¹ and 625 cm⁻¹. The phonon assignments of 4H and 9R BaRuO₃ are summarized in TABLE I.

On the other hand, Quilty et al.,¹⁸ from the c-axis measurement of 9R BaRuO₃, assigned the A_{1g} (Ru) mode at 280 cm⁻¹ as another O (E_g) mode. We note, as we will discuss later, that T-dependence of this mode and its frequency are quite similar to those of the A_{1g} (Ru) mode in 4H BaRuO₃. So, it is very likely that the mode at 280 cm⁻¹ is assigned as a A_{1g} (Ru) mode. It might be possible that a weak E_g (O) and a strong A_{1g} (Ru) mode are at nearly the same frequency.

B. T-dependent phonon spectra

Figures 3 (a) and 3 (b) show the T-dependent polarized spectra of 4H and 9R BaRuO₃, respectively. The spectra are shifted up for clarity. It is observed that both compounds show similar phonon spectra. Except for the E_{2g} (O) mode near 245 cm⁻¹ in 4H BaRuO₃, ve distinct phonon modes are observed at similar frequencies in both compounds. The A_{1g} and E_{2g} modes of 4H BaRuO₃ cor-

respond to the A_{1g} and E_g modes of 9R BaRuO_3 , respectively. It is noted that the corresponding phonon modes in both ruthenates show similar T-dependent behavior.

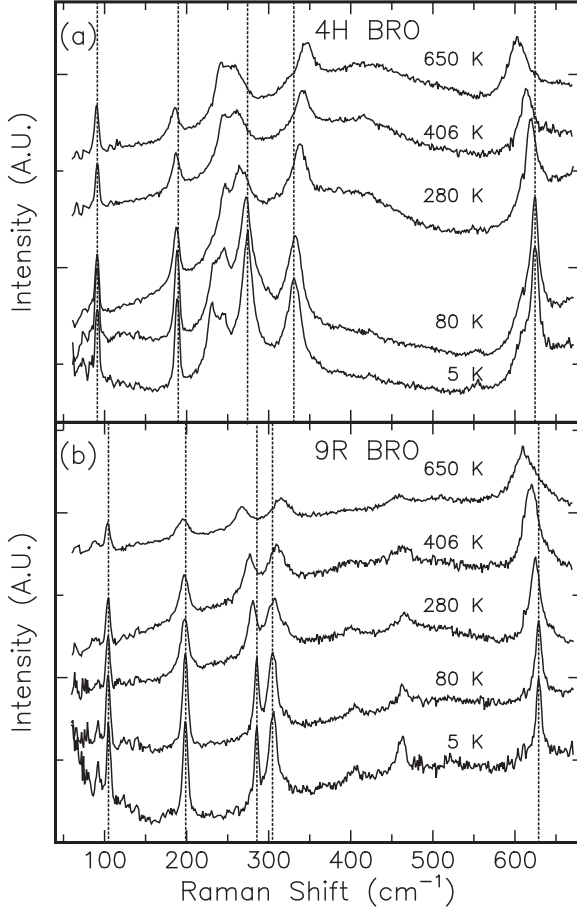


FIG. 3. Temperature-dependent polarized spectra of (a) 4H and (b) 9R BaRuO_3 in the ab -plane. The spectra are shifted up for clear presentation. The dotted lines are for guidance.

The A_{1g} modes show different T-dependent behavior from the E_{2g} (E_g) modes in both compounds. First, the A_{1g} (Ru) mode near 620 cm^{-1} and the A_{1g} (O) mode near 270 cm^{-1} strongly shift to higher frequencies with decreasing T. [The A_{1g} (Ba) mode in 9R BaRuO_3 shows a relatively weak hardening.] On the contrary, the E_{2g} (O) mode in 4H BaRuO_3 near 340 cm^{-1} and the E_g (O) mode in 9R BaRuO_3 near 300 cm^{-1} show a strong softening at lower T. These softenings are quite unusual in that the general T-dependent behavior of phonons is to show a hardening at lower T due to anharmonicity of lattice vibrations. Even in a quite wide T variation by 650 K , the E_{2g} (Ba, Ru) mode in 4H BaRuO_3 and E_g (Ba, Ru) mode in 9R BaRuO_3 show a very small change. On the other hand, as shown in Fig. 3(b), another E_{2g} (O) mode near 245 cm^{-1} , which is present only in the 4H BaRuO_3 , shows an anomalous T-dependence. This mode splits into two modes at low T. [The details will be discussed

in the next section.]

Figure 4 shows the detailed T-dependence of the phonons. The left panels, Figs. 4 (a), (b), (c), and (d) show the T-dependences of the A_{1g} (O), E_{2g} (O), A_{1g} (Ru), and E_{2g} (Ru) modes, respectively, of 4H BaRuO_3 . The right panels, Figs. 4 (e), (f), (g), and (h) show the T-dependence of the phonons of 9R BaRuO_3 corresponding to those of 4H BaRuO_3 , in sequence. While A_{1g} (O) modes show strong hardenings, E_{2g} (O) (or E_g) modes show softenings with decreasing T. Similarly, A_{1g} (Ru) modes show strong hardenings, but no significant change of E_{2g} (Ru) (or E_g) modes is observed. It is clear that A_{1g} modes show different T-dependent behavior from E_{2g} (E_g) modes.¹⁹

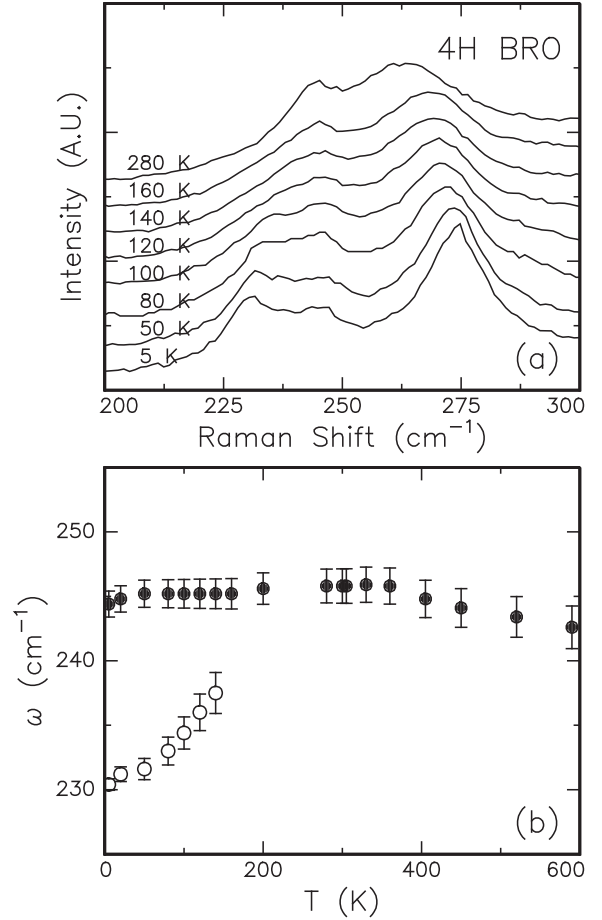


FIG. 4. The temperature-dependence of the phonon frequencies of (a) A_{1g} (O), (b) E_{2g} (O), (c) A_{1g} (Ru), and (d) E_{2g} (Ru) in 4H BaRuO_3 . (e) A_{1g} (O), (f) E_g (O), (g) A_{1g} (Ru), and (h) E_g (Ru) in 9R BaRuO_3 .

It is noted that the T-dependent behavior of the phonon modes closely depends on the direction of lattice vibrations. As a tentative description, E_g (or E_{2g}) and A_{1g} modes are related to the vibrations in the ab -plane and along the c -axis, respectively. The different T-dependence of the A_{1g} and E_{2g} (or E_g) modes could originate from their anisotropic structural properties with the

face-sharing of RuO_6 octahedra along the c -axis, through which a strong anisotropic interaction, i.e. a direct Ru metal bonding, occurs.

The strong hardenings of A_{1g} modes indicate that the bonding stiffness along the c -axis becomes larger. This also implies that the interaction along the c -axis, i.e. a direct Ru metal bonding, becomes stronger. It is noted that strong hardenings of A_{1g} modes cannot be simply explained by the variation of the c -axis lattice constant c . The A_{1g} modes vibrating along the c -axis are expected to have a close relation with c . However, while synchrotron XRD experiments with 4H-BaRuO_3 report that its c is changed just by 0.005 \AA with T varying between 30 K and 310 K ,²⁰ the phonon frequency ω_{ph} of the A_{1g} modes is changed by 10 cm^{-1} in the corresponding T range. These changes of the $\omega_{\text{ph}}(A_{1g})$ are much larger than those of the cuprates, where the stretching modes in Cu-O planes are quite sensitive to Cu-O bonding distances; while the lattice constant in the ab -plane is reduced by about 0.1 \AA , the ω_{ph} increases higher by 100 cm^{-1} .²¹ The relatively large change of the $\omega_{\text{ph}}(A_{1g})$ in BaRuO_3 system means that there must be another electronic contribution to the strong hardening of the A_{1g} modes in addition to those of the lattice effect.²² It is noted that similar hardening of the phonon modes in some manganites are observed due to charge ordering fluctuation.²³ On the other hand, in the infinite 1D chain cuprates, i.e. $\text{Ca}_{2-x}\text{Sr}_x\text{CuO}_3$, Drechsler et al. suggested the possible existence of a dynamic Peierl-type distortion and predicted phonon anomalies such as a hardening or a splitting.²⁴ The strong hardenings of the A_{1g} modes in the 1D-like ruthenates might be related to the CDW fluctuation by the metal bonding.

Unlike the A_{1g} modes, E_{2g} (or E_g) modes vibrating normally to the metal bonding direction show softenings or no significant change. Especially, strong softenings of the $E_{2g}(O)$ (or E_g) modes are quite unusual. It is noted that only the oxygens participating in the face-sharing have Raman-active modes. So, the softenings of the $E_{2g}(O)$ (or E_g) modes indicate that the bonding stiffness among the face-shared oxygens reduces and that there should be a kind of structural instability in the face-shared O structure. This also implies that the Ru-O-Ru interaction weakens as a Ru-Ru interaction strengthens, which could induce the stronger 1D-character. These differences in T -dependence between A_{1g} and E_g (E_{2g}) modes in BaRuO_3 could be a unique feature reflecting a structural instability due to the increase of the metal bonding strength.²⁵

C. Splitting of $E_{2g}(O)$ mode in 4H-BaRuO_3

Another important observation is that the $E_{2g}(O)$ mode near 245 cm^{-1} in 4H-BaRuO_3 shows a clear splitting. It is noted that this $E_{2g}(O)$ mode is not permitted in 9R-BaRuO_3 from group theory analysis. As shown

in Fig. 5(a), as T decreases, the $E_{2g}(O)$ mode becomes suppressed and a new mode at lower frequency develops. Together with the softenings of other $E_{2g}(O)$ modes, this splitting clearly indicates the existence of a structural instability in the face-shared structure. While the onset temperature of the phonon splitting is not clear, as shown in Fig 5(b), some anomaly is observed at 360 K , where the T -dependence of the $E_{2g}(O)$ mode is changed. This appears consistent with the optical observation that the pseudogap feature is still observed at 300 K .² It is very likely that this structural instability is closely related to the origin of the pseudogap formation in the ruthenates, i.e. the CDW instability.

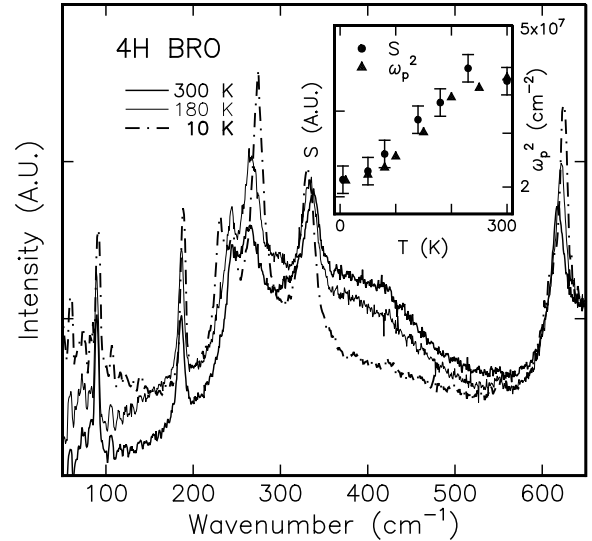


FIG. 5. (a) Temperature-dependent behavior of $E_{2g}(O)$ mode in 4H-BaRuO_3 . (b) Phonon frequency vs. temperature. The solid and open circle symbols represent the $E_{2g}(O)$ mode and a new phonon mode, respectively.

It is noted that the phonon splitting happens in the $E_{2g}(O)$ mode vibrating normally to the metal bonding direction. The splitting of an IR-active phonon mode in the ab -plane was also observed for a static CDW 9R-BaRuO_3 .⁶ This implies that the charge modulation along the c -axis might be closely related to the structural instability in the ab -plane. On the other hand, it is interesting that only the $E_{2g}(O)$ mode near 245 cm^{-1} shows the splitting. This means that the local structural distortion related to this mode occurs, maintaining the total crystallographic symmetry of the 4H compound. More theoretical and experimental studies are needed to understand the unusual CDW instability and its detailed relation to the pseudogap formation.

D. Electronic Raman continua

Electronic Raman continua give important information about the electronic excitation. Figure 6 shows T -

dependent polarized spectra of 4H BaRuO₃. As T decreases, Raman continua below 200 cm⁻¹ increase. This behavior is commonly observed in polarized and depolarized spectra in both ruthenates. The increase of Raman continua in low frequency region could be due to the reduction of the screening of free carriers on elastic scatterings, such as Rayleigh responses. This is consistent with optical observations that a reduction of carrier density occurs with pseudogap formation.^{1;2} Similar behavior was observed in some perovskite manganites with the metal-insulator transition.²⁶

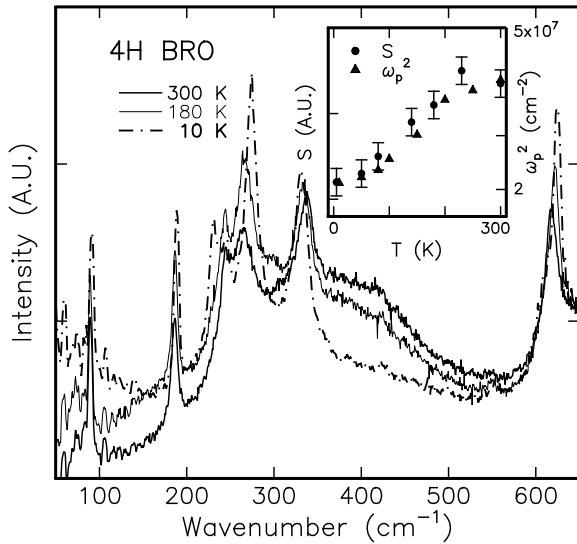


FIG. 6. Temperature-dependent Raman spectra of the 4H BaRuO₃ in the polarized direction. Inset: the solid circle and the solid triangle symbols represent the integrated Raman backgrounds S and the square of the plasma frequency ω_p^2 (quoted from Ref. [2]).

Another important point is that a broad Raman continuum near 400 cm⁻¹ in 4H BaRuO₃ is observed with a significant T -dependence.²⁷ As shown in Fig. 6, this broad continuum becomes suppressed with decreasing T . Because the maximum of the continuum is at a relatively high frequency, it cannot be an electronic Raman scattering by charge fluctuations arising from electron-hole excitations near the Fermi energy.²⁸ And, its position is different from that of the pseudogap position, 650 cm⁻¹.² To get qualitative physical insights, we integrated the Raman backgrounds in the frequency region of 250–600 cm⁻¹, where the T -dependence is dominant.²⁹ Interestingly, as shown in the inset of Fig. 6, the integrated area S is strongly correlated with the square of the plasma frequency ω_p^2 , obtained by optical measurement.² The reduction in ω_p^2 originates mainly from a reduction in n caused by a partial-gap opening on the Fermi surface. The strong correlation between S and ω_p^2 indicates that the suppression of the distinct Raman excitation near 400 cm⁻¹ might be closely related to the pseudogap formation.

IV. SUMMARY

Raman spectra in 4H and 9R BaRuO₃ show interesting features related to the metal-bonding formed through the face-sharing of RuO₆ octahedra. The temperature-dependence of the observed phonons strongly depend on the vibration direction with respect to the metal-bonding. For 4H BaRuO₃, another E_{2g} mode of the oxygen participating in the face-sharing is split clearly. The temperature-dependence of the broad electronic Raman continua near 400 cm⁻¹ suggests a partial-gap opening on the Fermi surface. These observations indicate that there occurs a kind of structural instability due to the metal-bonding, which could be closely related to the pseudogap formation in the BaRuO₃ systems.

ACKNOWLEDGMENTS

We acknowledge Jaejun Yu at Seoul National University for his helpful discussions. This work was supported by KOSEF through CSCMR. T.W.N. acknowledges Ministry of Science and Technology for financial supports through the Creative Research Initiative program. EJO and ISY acknowledge the support from the grant (No. KRF2000-015-D S0014) of Basic Science Research Institute program of the Korea Research Foundation.

e-mail: yslee@physa.snu.ac.kr

^z Present address: Department of Physics and Astronomy, University of Kentucky, Lexington, KY 40506.

^y Corresponding author, e-mail: yang@mm.ewha.ac.kr

¹ Y. S. Lee, J. S. Lee, K. W. Kim, T. W. Noh, Jaejun Yu, E. J. Choi, G. Cao, and J. E. Crow, Europhys. Lett. 55, 280 (2001).

² Y. S. Lee, J. S. Lee, K. W. Kim, T. W. Noh, Jaejun Yu, Yunkyu Bang, M. K. Lee, and C. B. Eom, Phys. Rev. B 64, 165109 (2001).

³ J. T. Rijssenbeek, R. Jin, Yu. Zadorozhny, Y. Liu, B. Batlogg, and R. J. Cava, Phys. Rev. B 59, 4561 (1999).

⁴ P. A. Cox, Transition metal oxides (Clarendon press, Oxford, 1992).

⁵ P. Khalifah, K. D. Nelson, R. Jin, Z. Q. Mao, Y. Liu, Q. Huang, X. P. A. Gao, A. P. Ramirez, and R. J. Cava, Nature (London), 411, 669 (2001).

⁶ G. Cao, J. E. Crow, R. P. Guertin, P. F. Henning, C. C. Homes, M. Strongin, D. N. Basov, and E. Lochner, Solid State Commun. 113, 657 (2000).

⁷ Recent synchrotron X-ray diffraction experiments with the c -axis oriented 4H BaRuO₃ epitaxial film report no superlattice peak. [Ref. 20]

⁸ Y. S. Lee, T. W. Noh, H. S. Choi, E. J. Choi, H. Eisaki, and S. Uchida, Phys. Rev. B 62, 5285 (2000).

- ⁹ G. Blumberg, M. V. Klein, and S.-W. Cheong, Phys. Rev. Lett. 80, 564 (1998).
- ¹⁰ Y. Lin and J. E. Eldridge, Phys. Rev. B 58, 3477 (1998).
- ¹¹ D. N. Argyriou, H. N. Bordallo, B. J. Campbell, A. K. Cheetham, D. E. Cox, J. S. Gardner, K. Hanif, A. dos Santos, and G. F. Strouse, Phys. Rev. B 61, 15269 (2000).
- ¹² M. K. Lee, C. B. Eom, W. Tian, X. Q. Pan, M. C. Smoak, F. Tsui, and J. J. Krajewski, Appl. Phys. Lett. 77, 364 (2000).
- ¹³ M. Shepard, S. McCall, G. Cao, and J. E. Crow, J. Appl. Phys. 81, 4978 (1997).
- ¹⁴ J. Y. Kim, S. Y. Lee, I. S. Yang, T. G. Lee, S. S. Yom, K. Kim, J. H. Kim, Physica C 308, 60 (1998).
- ¹⁵ P. C. Donohue, L. Katz, and R. Ward, Inorganic Chemistry 4, 306 (1965).
- ¹⁶ P. C. Donohue, L. Katz, and R. Ward, Inorganic Chemistry 5, 335 (1966).
- ¹⁷ M. Cardona and G. Guntherodt, Light scattering in Solids II (Springer-Verlag, Berlin, Heidelberg, New York, 1982).
- ¹⁸ J. Quilty, H. J. Trodahl, and A. Edgar, Solid State Commun. 86, 369 (1993).
- ¹⁹ Most of the phonon modes don't show any distinguishable anomaly in their width parameters, but instead a normal sharpening due to the reduction of a thermal fluctuation with decreasing T.
- ²⁰ J. H. Park, K. B. Lee, M. K. Lee, and C. B. Eom, to be published.
- ²¹ S. Tajima, T. Ido, S. Ishibashi, T. Itoh, H. Eisaki, Y. Mizuo, T. Arima, H. Takagi, and S. Uchida, Phys. Rev. B 43, 10496 (1991).
- ²² K. H. Kim, J. Y. Gu, H. S. Choi, G. W. Park, and T. W. Noh, Phys. Rev. Lett. 77, 1877 (1996).
- ²³ H. J. Lee, K. H. Kim, J. H. Jung, T. W. Noh, R. Surayanarayanan, G. Dhalenne, and A. Revcolevschi, Phys. Rev. B 62, 11320 (2000).
- ²⁴ S. L. Drechsler, J. M. Alek, M. Y. Lavrentiev, and H. Koppel, Phys. Rev. B 49, 233 (1994).
- ²⁵ The previous optical studies suggested that T₀ should be 430 K for 9R BaRuO₃ and above 300 K for 4H BaRuO₃. In our Raman spectra, weak anomalies in the T₀ region of 350 K–450 K are observed in both BaRuO₃ materials.
- ²⁶ S. Yoon, H. L. Liu, G. Schollerer, S. L. Cooper, P. D. Han, D. A. Payne, S.-W. Cheong, Z. Fisk, Phys. Rev. B 58, 2795 (1998).
- ²⁷ This electronic background is observed only in polarized spectra. This indicates that the Raman excitation might be related to an intraband transition within the conduction Ru 4d band. This background is hardly observed in 9R BaRuO₃ with a smaller n than 4H BaRuO₃.
- ²⁸ M. V. Klein and S. B. Dierker, Phys. Rev. B 29, 4976 (1984).
- ²⁹ It is assumed that the intensities of the phonons are not changed with T variation.

TABLE I. Summaries of the Raman-active phonon modes in 4H and 9R BaRuO₃ at 300 K.

4H BaRuO ₃			9R BaRuO ₃		
mode	frequency (cm ⁻¹)	assignment	mode	frequency (cm ⁻¹)	assignment
			A _{1g}	85	Ba
E _{2g}	91	Ba	E _g	105	Ba
E _{2g}	187	Ru	E _g	199	Ru
E _{2g}	245	O			
A _{1g}	264	Ru	A _{1g} (E _g)	282	Ru (O)
E _{2g}	339	O	E _g	307	O
			E _g	403	O
			A _{1g}	463	O
A _{1g}	619	O	A _{1g}	625	O